A&A manuscript no.
(will be inserted by hand later)

Your thesaurus codes are:
06(08.03.1; 08.13.2; 08.16.4; 09.16.1)

ASTRONOMY
AND
ASTROPHYSICS
19.3.1996

Non-spherical dust driven winds of slowly rotating AGB stars

E.A. Dorfi and S. Höfner

Institut für Astronomie der Universität Wien, Türkenschanzstr. 17, A–1180 Wien, Austria

Received date ....; accepted date ....

Abstract. We propose a new mechanism to explain an asymmetric mass loss for C-rich asymptotic giant branch (AGB)-stars based on the effect how rotation modifies dust driven winds. Even small deviations from spherical symmetry introduced by slow rotations are amplified in the zone of dust condensation due to the non-linear behaviour and the strong temperature and density dependence of the dust formation process. This mechanism leads to a preferential mass loss with higher velocities in the equatorial plane. Depending on the rotation rate we calculate for typical AGB stars stationary dust driven winds and present the rotation modulated solutions as a function of the polar angle. The mass loss rate can differ by large factors comparing the polar to the equatorial region. This mechanism provides also a simple explanation for the widely observed asymmetries found in the shapes of planetary nebulae.

Key words: Stars: carbon – mass loss – AGB and post-AGB, planetary nebulae: general

1. Introduction

Dust driven winds of C-rich AGB-stars are a widespread phenomenon since the radiation pressure on the newly formed dust grains provides an effective mechanism to accelerate the stellar material and to drive a slow but massive wind with typical velocities of $u_\infty \simeq 15\,\mathrm{km\,s^{-1}}$ and mass loss rates up to $\dot{M} \simeq 10^{-5} M_\odot\,\mathrm{yr}^{-1}$ (e.g. Lafon & Berruyer 1991). Based on self-consistent models of such dust driven winds it has become clear that a full treatment of the coupled system of time-dependent dust formation, radiation and gas dynamics is essential to describe the structure of the circumstellar envelope (e.g. Fleischer et al. 1992, 1995; Höfner et al. 1995). The process of dust formation depends strongly on the density and temperature stratification in the extended atmosphere and even small changes e.g. in the density at a given temperature can result in a totally different behaviour of the stellar wind. Either a stationary outflow develops with a lower degree of condensation or a so-called dust-induced κ-mechanism leads to a time-dependent wind with dense shells propagating outwards (Fleischer et al. 1995, Höfner et al. 1995).

Keeping this strong dependence of the dust formation process on density and temperature in mind we want to illustrate in this contribution the influence of a slow stellar rotation on dust driven outflows. According to theoretical estimates on magnetic braking of stars as well as observations of atmospheric velocities the angular velocity decreases with the stellar age. Hence, for the luminous late type stars we expect only slowly rotating objects where the deviations from spherical symmetry are small quantities. However, an exceptional object like V Hyd (Barnbaum et al. 1995) has been observed showing a bipolar outflow together with a high rotational velocity. It is believed that such a rapid rotation of an AGB star is due to spin-up by a companion in a common envelope configuration. For such a case we find a very strong angular dependence of the mass loss for the proposed mechanism but already small rotational velocities of the order of $2\,\mathrm{km\,s^{-1}}$ at the stellar photosphere cause significant variations in the outflow velocities and the mass loss. Such an asymmetric mass loss during the AGB phase could explain the bipolar appearance of many planetary nebulae (PNe) according to interacting wind models (e.g. Kwok 1982, Kahn & West 1985). However, concerning the final shape of the developing PN it could be that also different mechanisms are responsible for the bipolar morphology observed in various PNe.

Preliminary results have been presented by Dorfi and Höfner (1995) but the extended envelopes of these luminous late type stars have been calculated without solving the full system of radiation hydrodynamics. Adopting the Lucy-approximation (Lucy 1971, 1976) the temperature stratification has been obtained as a function of the density ρ and the gas and dust opacities. Although these approximate solutions reveal basic changes in the dust driven winds due to the stellar rotation a number of differences are found compared to this full treatment since only the effects of the opacity changes have been included. As discussed in the following sections several effects, namely the centrifugal force, the degree of particle condensation as well as the modifications in the outflow velocities contribute in various ways to change the behaviour of dust driven winds.

Send offprint requests to: E.A. Dorfi
e-mail: ead@astro.ast.univie.ac.at

2. Physical model and assumptions

According to observations all old stellar objects exhibit only small rotational velocities (e.g. Slettebak 1970) because during the whole stellar life magnetic fields link the stellar body to the external medium providing together with a stellar wind a natural braking mechanism. For the red giants on the asymptotic giant branch (AGB) we can therefore consider only tiny deviations from radial symmetry and deal with almost spherical configurations. In such cases it is common to assume that all basic physical quantities are constant on equipotential surfaces and only the radiative flux varies with the angle from the axis (e.g. Tassoul 1978).

2.1. Influence of stellar rotation

The inclusion of rotation causes two effects on the star, namely a global expansion due to the centrifugal force as well as a departure from sphericity due to a non-spherical part of the effective gravity. Moving from the stellar surface to the zone of dust formation we are faced with a slightly different scale height in the atmosphere and also small variations of the radiative flux along the polar angle.

For the case of slow rotations the so-called quasi-spherical approximation is sufficient to describe the non-spherical effects. Working with a mean radius this method has been incorporated in standard stellar evolution calculations (e.g. Kippenhahn et al. 1970). An additional term accounts for centrifugal acceleration a_ω in the equation of motion, i.e.

$$a_\omega = \omega^2 s, \qquad \text{and} \qquad s = r\sqrt{1-\mu^2} \tag{1}$$

and s stands for the distance from the axis of rotation, r denotes the radius and $\mu = \cos\theta$ with the polar angle θ. In the following sections most plots show the physical variables as functions of μ. The discretization of this term is straightforward and all the details of our numerical scheme can be found for the dust equations in Dorfi and Höfner (1991) and for the radiation hydrodynamics in Dorfi and Feuchtinger (1995), respectively.

Taking into account only slow rotations the outer stellar layers are approximated by a rotating polytrope with a polytropic index of $n = 3/2$ which is appropriate for fully convective stars. The interior structure of an AGB-star is largely simplified by this procedure since it neglects the White Dwarf in the central region as well as the burning shells. However, these polytropic description allows a simple determination of the contour of the stellar boundary $r_b(\theta)$ relevant to our problem. We need the angle dependence of the radius to place our inner boundary conditions. Calculating an initial hydrostatic model we specify all physical quantities at these locations $r_b(\theta)$ as a function of the polar angle θ. The radiative flux varies according to the effective gravity (e.g. Tassoul 1978) and at this level of approximation all other physical quantities are constant on this equipotential surface. The contour $r_b(\theta)$ is expanded in terms of the small parameter

$$v = \frac{\omega^2}{2\pi G\rho_c} \tag{2}$$

where ρ_c denotes the central density and ω the angular velocity (e.g. Tassoul 1978). We obtain the central density from the theory of polytropes, i.e. $\rho_c/\bar{\rho} = 5.99$ where the mean density $\bar{\rho} = 3M/4\pi R^3$ is easily calculated from our basic stellar parameters. Hence, taking a stellar luminosiy, a stellar mass, an effective temperature and an angular velocity we determine the inner boundary conditions as a function of the polar angle θ.

In order to keep the models as simple as possible we do not invoke any further transport of angular momentum during the outflow. Therefore we take the specific angular momentum to be constant, i.e. $\omega^2 s = const$. Applying this assumption it is clear that $a_\omega \propto r^{-3}$ when the material flows outwards and that the gravitational decceleration is only overcome by the radiation pressure on the newly formed dust grains.

2.2. Dust formation

The complicated interactions between the thermodynamical conditions and dust formation in a dust-driven stellar wind require a detailed time-dependent treatment of the dust component. On the one hand the thermodynamics and chemistry of the gas phase determine the grain formation and growth, i.e. the abundance and size spectrum of the dust particles. On the other hand the acceleration of the dust-gas-mixture by radiation pressure and the backwarming caused by the high opacity of the grains influences the conditions in the dust-forming region of the extended atmosphere.

We consider the formation and growth of amorphous carbon grains by solving the so-called moment equations (Gail & Sedlmayr 1988, Gauger et al. 1990) together with the equations of radiation-hydrodynamics. They describe the time evolution of an ensemble of dust grains in terms of moments of the grain size distribution which are related to means of the grain radius. The number densities of the relevant molecules (e.g. C, C_2, C_2H and C_2H_2) are calculated assuming chemical equilibrium and the formation of small nuclei is described by a thermodynamical nucleation rate generalized to heteromolecular reactions. For further details about the physical input see Höfner et al. (1995) and references therein. Note that the grain opacity is the same as in Höfner et al. (1996), i.e. $Q'_{\rm ext} = 4.4\,T_{\rm r}$ with $T_{\rm r}$ denoting the radiative temperature.

2.3. Stationary winds

Presently, we restrict our investigations to the case of stationary winds where the effects of the rotation can be seen more clearly than in the complicated situation of a time-dependent outflow. However, we have to keep in mind that these stationary models are somewhat artificial since most AGB stars are pulsating variables and furthermore – even for a non-variable star – the dust-driven outflow may be unstable due to the dust-induced κ-mechanism as demonstrated by Fleischer et al. (1995) and Höfner et al. (1995).

The models presented in Sect. 3 are obtained in the following way: First, starting from a non-rotating, hydrostatic and dust-free initial model we generate a stationary wind model with $\omega = 0$ as described in Höfner et al. (1995). In a second step – using this model as a starting point – we include the effects of rotation (the additional term in the equation of motion and the modified inner boundary conditions, cf. Sect. 2.1). The angle dependence of the outflow is then obtained by calculating a series of stationary solutions for a number of polar angles (usually 11). Such a treatment cannot account for the possible development of Kelvin-Helmholtz instabilities due to the θ-dependence of the radial ouflow velocities. However, in an expanding stellar wind the relevance of this instability seems to be rather limited.

Although we present only stationary flows in the next section we want to emphasize that all computations have been carried out by using the full time-dependent coupled equations of gas, dust and radiation. During the development towards a stationary solution perturbations are damped artificially by a limited temporal resolution of the calculation, i.e. allowing for large time steps to avoid the occurrence of the dust-induced κ-mechanism in the outflow (cf. Höfner et al. 1996).

3. Results

To demonstrate the effects of a slow stellar rotation on a dust-driven wind we choose the parameters of a well-studied model (case A of Höfner et al. 1995, 1996), i.e. $M = 1\,M_\odot$, $L = 10^4\,L_\odot$, $T_{\rm eff} = 2600$ K and $\varepsilon_{\rm C}/\varepsilon_{\rm O} = 2.3$. The results are summarized in Table 1 which contains also a second model with a slightly higher luminosity. Note, however, that the plots and results discussed in this section refer to the model with $L = 10^4 L_\odot$.

3.1. Radial structures

Figure 1 depicts the radial structure of the stellar wind having an angular velocity of $\omega = 2\,10^{-8}{\rm s}^{-1}$ for different polar angles. Each curve shows the familiar picture of a stationary dust-driven wind: the hydrostatic stellar atmosphere with its steeply decreasing density, the zone of dust condensation and radiative acceleration and, finally, the wind region.

The highest outflow velocities of $u_{\infty,{\rm e}} = 22\,{\rm km\,s}^{-1}$ (cf. Fig. 1a) and mass loss rates $\dot{M}_{\rm e}= 2\,10^{-6} M_\odot\,{\rm yr}^{-1}$ (as inferred from the densities, Fig. 1b) occur in the equatorial plane (full line) and both quantities decrease monotonically towards the polar direction. The same behaviour is found for the dust-to-gas mass ratio which can be deduced from the degree of condensation $f_{\rm c}$ (Fig. 1c), i.e. the fraction of condensible material (all carbon not bound in CO) actually condensed into grains. This dust-to-gas mass ratio varies between $1.1\,10^{-3}$ at the pole and $3.0\,10^{-3}$ at the equator.

To understand this strong dependence of the stellar wind on the polar angle we have to discuss the dust formation and driving mechanism of the outflow in some detail.

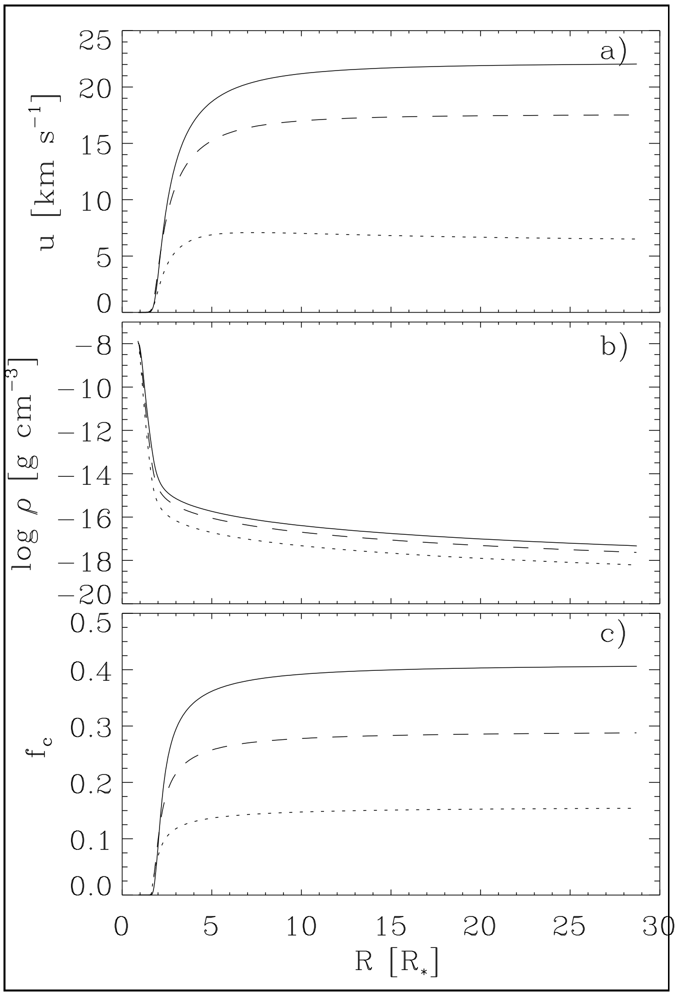

Fig. 1. The radial structure of a rotating stationary dust driven wind with a stellar angular velocity of $\omega = 2\,10^{-8}{\rm s}^{-1}$ plotted for three different angles, equatorial wind (solid line), 45 degrees (dashed line) and polar wind (dotted line); **a)** the gas velocity in units of [${\rm km\,s}^{-1}$] between 1 and 30 R_*, **b)** the gas density and **c)** the degree of condensation of carbon dust grains.

3.2. Dust formation efficiency

Apart from the chemical composition of the gas the grain formation and growth rates depend on the temperature and the density of the gas. The temperature largely determines the point where grain formation in principle becomes possible but the density controls the growth process of the dust particles.

In Fig. 2 the variation of the density (normalized to the equatorial value) is plotted as a function of the polar angle θ along three different isotherms in the atmosphere of the AGB-star. The temperatures chosen characterize different regions of the extended atmosphere and the wind: The innermost isotherm at 1700 K (dashed line) represents the dust-free hydrostatic atmosphere. Around 1500 K (dotted line) dust condensation becomes a decisive factor affecting the thermal and dynamical structure of the atmosphere. The third isotherm at 1300 K (full line) is located in the acceleration region of the stellar wind where a

Table 1. Table of results for two different stellar models (in both cases $M = 1\,M_\odot$ and $T_{\rm eff} = 2600$ K) and various angular velocities ω corresponding to a rotation period P: integrated mass loss rate $\dot{M}$, ratio of mass loss rates at the equator and the pole $\dot{M}_{\rm e}\,/\,\dot{M}_{\rm p}$, ratio of degrees of condensation at the equator and the pole $f_{\rm c,e}/f_{\rm c,p}$, final outflow velocity at the equator $u_{\infty,\rm e}$ and final outflow velocity at the pole $u_{\infty,\rm p}$.

L $[L_\odot]$	$\varepsilon_{\rm C}/\varepsilon_{\rm O}$ [C/O]	ω $[\rm s^{-1}]$	P [yr]	$v \sin i$ $[\rm km\,s^{-1}]$	$\dot{M}$ $[10^{-6} M_\odot\,\rm yr^{-1}]$	$\dot{M}_{\rm e}\,/\,\dot{M}_{\rm p}$	$f_{\rm c,e}/f_{\rm c,p}$	$u_{\infty,\rm e}$ $[\rm km\,s^{-1}]$	$u_{\infty,\rm p}$ $[\rm km\,s^{-1}]$
10^4	2.3	$2\,10^{-8}$	10	6.9	1.38	25.8	2.6	22.0	6.5
10^4	2.3	$1.5\,10^{-8}$	13	5.1	0.74	7.1	1.8	18.8	9.2
10^4	2.3	10^{-8}	20	3.4	0.44	2.6	1.3	15.6	10.9
10^4	2.3	$5\,10^{-9}$	40	1.7	0.31	1.3	1.1	13.1	11.9
10^4	2.3	10^{-9}	200	0.3	0.29	1.0	1.0	12.3	12.2
10^4	2.3	0.0	∞	0.0	0.29	1.0	1.0	12.3	12.3
$1.2\,10^4$	2.0	10^{-8}	20	3.8	0.65	3.2	1.4	12.9	8.1
$1.2\,10^4$	2.0	10^{-9}	200	0.4	0.38	1.0	1.0	9.5	9.5
$1.2\,10^4$	2.0	0.0	∞	0.0	0.38	1.0	1.0	9.5	9.5

significant fraction of the final degree of condensation has already been reached and the spatial structure is dominated by the outflow.

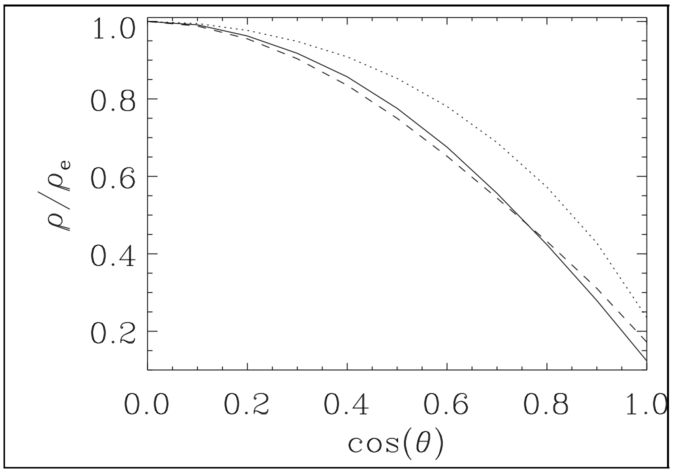

Fig. 2. The gas density normalized to the density in the equatorial region as a function of the polar angle θ for three different temperatures (full line: 1300 K, dotted line: 1500 K, dashed line: 1700 K).

The rotation parameter is set to $v = 0.02$ which corresponds to an angular velocity of $\omega = 2\,10^{-8}\rm s^{-1}$ or a rotation period of $P = 10$ years. At the stellar photosphere of 493 $R_\odot$ the maximum rotation velocity $v \sin i$ is then $6.9\,\rm km\,s^{-1}$ and the ratio of the equatorial radius to the polar radius is 1.09. In this case all lines showing the decrease of the gas density on isotherms exhibit a variation of about a factor of 10 as going from the equator towards the pole. Such a strong dependence on the polar angle efficiently influences the dust formation process since

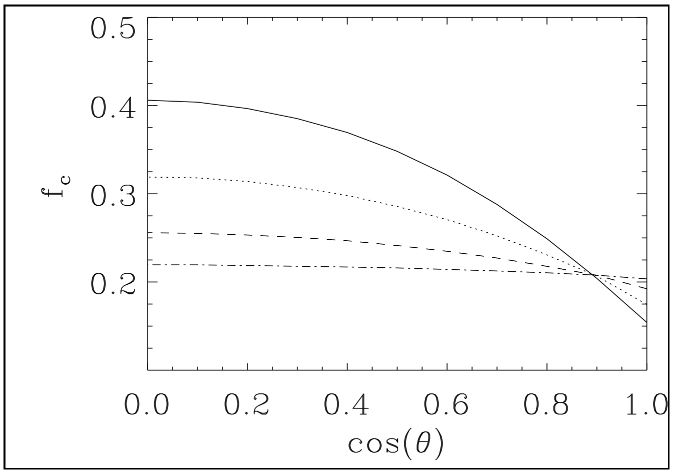

Fig. 3. The degree of condensation as a function of the polar angle θ for four different angular velocities (full line: $\omega = 2\,10^{-8}\rm s^{-1}$, dotted line: $\omega = 1.5\,10^{-8}\rm s^{-1}$, dashed line: $\omega = 10^{-8}\rm s^{-1}$, dashed-dotted line: $\omega = 5\,10^{-9}\rm s^{-1}$.

the main non-linearity and time-dependence of dust growth rate is determined by the density of the condensible material.

This effect is reflected in Fig. 3 (full line) showing the final degree of condensation $f_{\rm c}$ as a function of the polar angle. We find that a considerably higher fraction of material condenses into grains in the equatorial plane than in the polar direction. Note that the relative variation of $f_{\rm c}$ is slightly less than that of the isothermal density at 1500 K. The effect of a higher density at a given temperature (which in principle leads to more efficient dust condensation) may partly be compensated by a more rapid dilution of the condensible material due to a higher radiative acceleration.

3.3. Mass loss

As soon as a small fraction of the carbon has condensed into solid particles the high opacity of the grains leads to a considerable acceleration of the gas-dust-mixture by the strong radiation field of the star. The temperature and density of the outflowing gas decrease and gradually the grain growth stops due to the dilution of the condensible material in the stellar wind. The final values of f_c are far from unity (which would indicate complete condensation of all carbon not bound in CO).

The variation of the final outflow velocity as a function of $\cos(\theta)$ (Fig. 4) is a consequence of the behaviour of f_c (Fig. 3) since the dust opacity (and consequently the radiative pressure) is proportional to f_c.

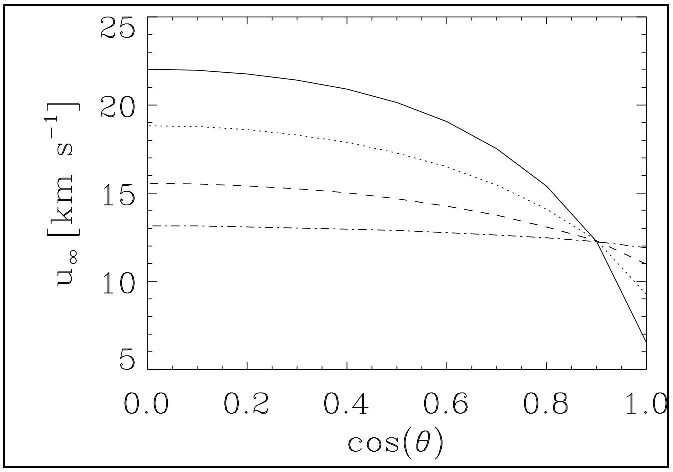

Fig. 4. The terminal velocity in units of [km s^{-1}] as a function of the polar angle θ for four different angular velocities (full line: $\omega = 2\,10^{-8}$s^{-1}, dotted line: $\omega = 1.5\,10^{-8}$s^{-1}, dashed line: $\omega = 10^{-8}$s^{-1}, dashed-dotted line: $\omega = 5\,10^{-9}$s^{-1}.

The mass loss rate (Fig. 5) shows a strong dependence on the polar angle. The quantity plotted depicts the effective mass loss rate which is the differential mass loss rate multiplied by the corresponding spherical surface to obtain familiar units. This ratio of the mass loss rates at the equator and the pole is much larger than the ratio of the outflow velocities. This again reflects the influence of the rotation on the density in the wind acceleration region (cf. Figs. 1b and 2).

4. Discussion

A large number (> 50%) of planetary nebulae show a pronounced aspherical shape (Zuckerman & Aller 1986) and a number of models (e.g. Morris 1990 for a review) have been proposed to explain this asymmetry by rotation of the central star (Mufson & Liszt 1975, Phillips & Reay 1977), an intranebular magnetic field (Pascoli 1987) or by binarity (Eggleton 1990, Morris 1987, Soker & Livio 1989). However, in contrast to these models the results presented in the previous sections give a different view since rotation provides only a small perturbation of

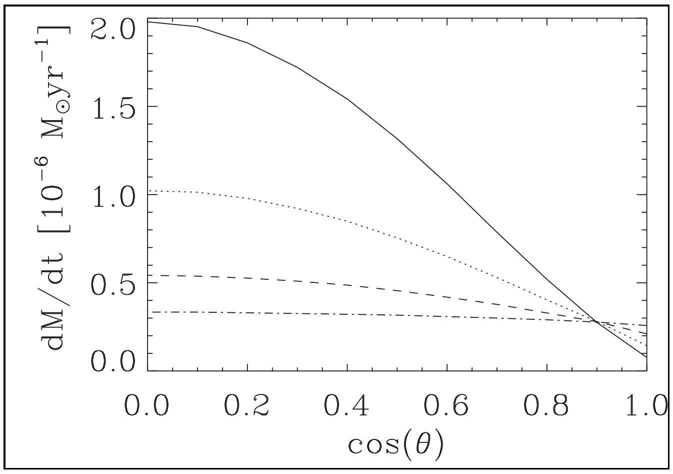

Fig. 5. The effective mass loss rate in units of [$10^{-6} M_\odot$ yr^{-1}] as a function of the polar angle θ for four different angular velocities (full line: $\omega = 2\,10^{-8}$s^{-1}, dotted line: $\omega = 1.5\,10^{-8}$s^{-1}, dashed line: $\omega = 10^{-8}$s^{-1}, dashed-dotted line: $\omega = 5\,10^{-9}$s^{-1}.

the stellar surface which is then amplified by the non-linearities occurring in the dust forming region.

A theoretical explanation for the shaping of planetary nebula is based on the interacting stellar winds model (Kwok 1982) where a spherical fast wind blows into a previously asymmetric slow wind of the red giant (Kahn & West 1985). The mass loss rates obtained by our calculations (cf. Fig. 5) can be fitted with their assumed angle-dependent mass loss rates of

$$\dot{M}\,(\theta) = \dot{M}_{\rm p}\,(1 + \varepsilon \sin^n \theta) \qquad (3)$$

with $\varepsilon = \dot{M}_{\rm e} \;/\; \dot{M}_{\rm p} - 1$ and $n \simeq 2 \ldots 3$. Taking these values the shapes of planetary nebulae become quite asymmetric if the ratio of the mass loss rate $\dot{M}_{\rm e} \;/\; \dot{M}_{\rm p}$ is larger than a factor of 2. Recent observations of protoplanetary nebulae showing axial rather than spherical symmetry (Skinner et al. 1995) seem to support this scenario. As the star evolves and looses mass the angular momentum distribution inside the star determines the angular dependence of the mass loss as long as enough dust particles condense and provide the main driving mechanism of the stellar wind.

Taking as a typical example a slow rotating red giant ($T_{\rm eff}$ = 2600 K, $M = 1\,M_\odot$, $L = 10^4 L_\odot$) with a photospheric rotational velocity of about 2 km s^{-1} we can state several important points by comparing the results to the case of a non-rotating AGB star. First, the total mass loss rate increases by a factor of 1.5 relative to the mass loss of the non-rotating star. Secondly, the mass loss in the equatorial plane is about 2 times larger than in the polar direction. Thirdly, the terminal velocity increases from 11 km s^{-1} to 15 km s^{-1} as going from the pole towards the equator. As demonstrated in the previous sections these changes are due to the modifications of the dust formation process introduced by the small rotational velocities at the stellar atmosphere.

Since convection acts as an additional dissipation mechanism it is likely that fully convective regions exhibit a rigid rotation. However, this result is strictly valid only for the limit of an isotropic convection but in a rotating star the angular momentum reduces the efficiency of convective transfer with increasing latitude (Biermann 1951, Roxburgh 1974). The existence of meridional circulations in a convective zone of rotating stars (Taylor 1973) favors the transport of angular momentum towards the equator even for small rotation rates (Durney 1970). Since both effects lead to larger differences between the polar and the equatorial zones relative to the case of rigid rotation the models presented here give lower limits for the influence of rotation on dust driven winds.

Since the development of stationary solutions in a non-pulsating red giant depends critically on the density and temperature stratification in the dust forming zone it is very likely that these flows are subject to the so-called dust-induced κ-instability (Fleischer et al. 1995, Höfner et al. 1995). However, in the case of a rotating AGB star the occurrence of a such time-dependent dust formation is then a function of the polar angle. Although the dust induced κ-instability is more likely to begin in the equatorial region the excited oscillations can propagate towards higher latitudes triggering variations of the polar outflow. If the rotational velocity increases the ratio of equatorial mass loss to the polar mass loss increases by large factors, e.g. a factor of 25.8 for a rotation period of 10 years (cf. Table 1). A large rotational velocity also reduces the density in the polar region and therefore we enter the regime where only a few dust particles can condense and where the radiation pressure on these few particles is not sufficient to drive a stellar outflow. There exists a minimum mass loss rate for dust driven winds (Gail & Sedlmayr 1987). In the fastest rotating model (first line of Table 1 and solid line of Fig. 5) the polar mass loss rate is reduced to $\dot{M} = 7.7\,10^{-8} M_\odot\ \mathrm{yr}^{-1}$ which is close to such a limit. In general the overall flow structure will be complicated since the time scales of dust condensation differ for different polar angles which might explain the clumpyness as well as the departure from spherical symmetry observed at higher resolution in some of these outflows (e.g. Lucas et al. 1995).

5. Conclusions

Based on the aforementioned models we have shown in typical examples that changes of the gas density with respect to a given temperature are already present when the star slowly rotates. The small changes in the atmospheric layers lead to a larger variation in the dust forming time scales which clearly influences the behaviour of dust driven winds. Hence, we find a notable difference between the polar region and the equatorial plane even if the rotational velocities are almost undectable due to an intrinsinc temporal variability of these objects. Such a predominant mass loss in the equatorial plane during the AGB phase will affect the shaping of the resulting planetary nebula and favours a bipolar morphology. Although we have restricted the discussion to a stationary mass loss we are convinced that the mechanism proposed also works in the case of time-dependent dust driven winds of slowly rotating AGB stars.

Acknowledgements. This work is supported by the Österreichischer Fonds zur Förderung der wissenschaftlichen Forschung (FWF) under project number S7305-AST.

References

Barnbaum C., Morris M., Kahane C., 1995, ApJ 450, 862
Biermann L., 1951 Zeit. f. Astrophys. 28, 304
Dorfi E.A., Feuchtinger M.U., 1995, Comp. Phys. Comm. 89, 69
Dorfi E.A., Höfner S., 1991, A&A 248, 105
Dorfi E.A., Höfner S., 1995, Poster Proceedings: Stellar Surface Structure (IAU Symp 176), Ed. K.G. Strassmeier, Univ. of Vienna 1995, p. 226
Durney B.R., 1970, ApJ 161, 1115
Eggleton P.P., 1990, in Form Miras to Planetary Nebulae: Which Path for Stellar Evolution?, eds. M.O. Mennessier and A. Omont, Editions Frontières, Montpellier, p. 513
Fleischer A.J., Gauger A., Sedlmayr E., 1992, A&A 266, 321
Fleischer A.J., Gauger A., Sedlmayr E., 1995, A&A 297, 543
Gail H.-P., Sedlmayr, E., 1987, A&A 177, 186
Gail H.-P., Sedlmayr, E., 1988, A&A 206, 153
Gauger A., Gail H.P., Sedlmayr E., 1990, A&A 235, 345
Höfner S., Dorfi, E.A., 1992, A&A 265, 207
Höfner S., Feuchtinger M.U., Dorfi, E.A., 1995, A&A 297, 815
Höfner S., Fleischer A.J., Gauger A., Feuchtinger M.U., Dorfi E.A., Winters J.M., Sedlmayr E., 1996, A&A, submitted
Kahn F.D., West K.A., 1985, MNRAS 212, 837
Kippenhahn R., Meyer-Hofmeister E., Thomas H.C., 1970, A&A 5, 155
Kwok S., 1982, ApJ 258, 280
Lafon J-P.J., Berruyer N., 1991, A&AR 2, 249
Lucas R., Guélin M., Kahane C., Audinos P., Cernicharo J., 1995, Ap&SS 224, 293
Lucy L., 1971, ApJ 163, 95
Lucy L., 1976, ApJ 205, 482
Morris M., 1987, PASP 99, 1115
Morris M., 1990, in Form Miras to Planetary Nebulae: Which Path for Stellar Evolution?, eds. M.O. Mennessier and A. Omont, Editions Frontières, Montpellier, p. 520
Mufson S.L., Lizst H.S., 1975, ApJ 202, 183
Pascoli G., 1987, A&A 180, 191
Phillips J.P., Reay N.K., 1977, A&A 59, 91
Skinner C.J., Meixner M., Barlow M.J., Justtanont K., Arens J.F., Jernigan G., 1995, Ap&SS 224, 383
Slettebak A. (Ed.), 1970, IAU Symp. Stellar Rotation, Columbus, D. Reidel, Dordrecht
Soker N., Livio M., 1989, ApJ 339, 268
Roxburgh I.W., 1974, Ap&SS 27, 419
Tassoul J-L., 1978, Theory of Rotating Stars, Princeton Univ. Press, Princeton
Taylor R.J., 1973, MNRAS 165, 39
Zuckerman B., Aller L.W., 1986, ApJ 301, 772

This article was processed by the author using Springer-Verlag LaTeX A&A style file *L-AA* version 3.